URSI GASS 2021, Rome, Italy, 28 August - 4 September 2021

Analysis of the Radial PML in Cylindrical Finite Integration Technique Using a Hybrid Implicit-Explicit Update Scheme

Lilli Kuen(1) and Rolf Schuhmann(1)
(1) Technische Universität Berlin, Theoretische Elektrotechnik, EN-2, 10587 Berlin, Germany, http://www.tet.tu-berlin.de

Abstract

We study the performance of the Perfectly Matched Layer (PML) boundary technique within a Finite Integration/Finite Differences method for the simulation of electromagnetic waves in structures with rotational symmetry. To solve the stability issues of PML in time-domain which have been reported in literature, we have previously introduced a hybrid implicit-explicit algorithm. It applies a stabilizing implicit update scheme for components within the PML region only, but reduces to the standard explicit leapfrog method in the main computational domain. For a so-called 2.5-D grid in ρz-coordinates, this algorithm is extended to the PML in the ρ-direction, and its stability and accuracy properties are analyzed. The results show that the radial ρ-PML has less influence on the stability of the time integration compared to the longitudinal z-PML. Thus, it can be operated using the same parameters as longitudinal PML or even using standard leapfrog integration.

1 Introduction

Many simulations require absorbing boundary conditions, for example, the analysis of antennas or radiating components in microwave technology or optics. The Perfectly Matched Layer (PML) technique is the most common material based open boundary condition. It was first introduced in 1996 by J.-P. Bérenger [1] and is characterized by a frequency-independent formulation. This is especially useful for broadband time-domain simulations. The PML boundary features additional material layers at the boundary of the computational domain, which are filled with artificial conductivities (κ and σ) with a specific spatial profile. In the commonly applied anisotropic setup, the transversal conductivities are responsible for the absorption of incident waves, and the normal components provide the required impedance matching. There exist several different approaches for the implementation of this PML concept including its time discretization and the corresponding integration formulas.
However, it has been reported in literature [2, 3] that some of the implementation variants of the well-known leapfrog update method – the key idea of the FDTD method, applied to PML – can have stability problems. The occurring instabilities only weekly depend on the Courant criterion and can typically not be avoided simply by reducing the time step width. In a previous publication [4] we have already shown that the discretization of the time axis itself, regarding the additional PML equations, has an impact on the dynamic behavior of different time integration schemes and thus on the problems with stability. To obtain more degrees of freedom to influence the stability, a hybrid implicit-explicit algorithm has been introduced in [5]. The time integration follows the explicit leapfrog-like update equations for all components in the main computation area, whereas an implicit scheme is used inside the PML region.

In this paper, this scheme is applied to the absorbing PML boundary in the radial direction of a cylindrical computational grid. As a simple evaluation example, we analyze a hollow structure, where cylindrical waves are excited by a current source at its center and allowed to propagate in radial direction. This allows us not only to test the stability of the PML implementation but also to measure the practically reached reflectivity of the PML. The simulation is performed in Time Domain using the Finite Integration Technique (FIT) applied to a cylindrical grid, with the so-called Body of Revolution ansatz [6].

2 Basic Principles

2.1 Standard Leapfrog and PML

A staggered grid is used for the spatial discretization of the Finite Integration Technique (FIT) [6]. The resulting matrix-vector formulation consists of grid voltages $\widehat{\mathbf{e}}$ and $\widehat{\mathbf{h}}$, diagonal material matrices $\mathbf{M}_\mu$ and $\mathbf{M}_\varepsilon$, and the curl matrix $\mathbf{C}$, resp. FIT allows using the leapfrog time integration scheme

$$\widehat{\mathbf{h}}^{n+\frac{1}{2}} = \widehat{\mathbf{h}}^{n-\frac{1}{2}} - \Delta t \mathbf{M}_\mu^{-1} \mathbf{C} \widehat{\mathbf{e}}^n, \tag{1}$$

$$\widehat{\mathbf{e}}^{n+1} = \widehat{\mathbf{e}}^n + \Delta t \mathbf{M}_\varepsilon^{-1} \mathbf{C}^T \widehat{\mathbf{h}}^{n+\frac{1}{2}}. \tag{2}$$

Herein, the electric and magnetic degrees of freedom are sampled on full and half-time steps, respectively. The time derivatives are substituted by finite difference expressions with a time step width Δt. These equations are computationally equivalent to corresponding FDTD schemes, including the well-known proofs for conditional stability [6] (without PML).

The performance of the PML can be measured using the remaining (parasitical) reflection of outgoing waves, and is

typically controlled by two parameters: First, the number N_{lay} of additional grid layers defines the additional effort invested in the boundary condition. In combination with the longitudinal grid step width (constant within the PML and adopted from the last step width in the main domain), it defines the physical length provided by the PML to absorb the outgoing waves. Within this additional domain, the artificial conductivities follow a predefined profile which is quadratic in all our experiments. The slope of this profile is adjusted from some analytic considerations [1] to reach a certain maximum reflection $\mathscr{R}$ which constitutes the second control parameter.

Note that all those parameters have originally been defined based on plane waves in a Cartesian setup. In the cylindrical coordinates used here, with non-constant metric coefficients and cylindrical waves crossing a curved interface between the main domain and PML, it is no longer guaranteed that the standard choice of parameters is somehow optimal. Additionally, the achievable reflection in practical computations depends on the angle of incidence of the waves, which also leads to poor performance (up to the total loss of the wave absorption property) for guided waves close to cut-off. Finally, the spatial resolution of the grid has some influence.

Concerning the additional memory requirements of the PML, the computational area is increased by $N_{lay} \cdot N_z$ grid points for a ρ-PML. Since $N_r \gg N_{lay}$ usually applies, the relative increase in grid points is not too large. For a standard PML update, both Φ and Ψ need to store an old $\widehat{\mathbf{h}}$ and $\widehat{\mathbf{e}}$ vector inside the PML. The additional effort is therefore manageable.

2.2 Hybrid Time Update with ρ-PML

To obtain additional parameters to control the stability, an implicit algorithm in the PML region is used. Combining this with an explicit algorithm in the rest of the computational domain yields the hybrid implicit-explicit algorithm presented in [5] for a PML in the z-direction. In the case of a PML in ρ-direction, the deviation is analogous. The implicit method is obtained by substituting the electric grid voltages $\widehat{\mathbf{e}}$ in (1), by using the Newmark-beta ansatz [7]

$$\widehat{\mathbf{e}}^n \approx \beta \widehat{\mathbf{e}}^{n+1} + \left(\frac{1}{2} - 2\beta + \gamma\right) \widehat{\mathbf{e}}^n + \left(\frac{1}{2} + \beta - \gamma\right) \widehat{\mathbf{e}}^{n-1}. \quad (3)$$

The introduced parameters $\beta \in [0,1]$ and $\gamma \in [0,1]$ allow the weighting of different time instances (β) and a switch from forward and backward time stepping (γ). Herein, an implicit update with equations for electric and magnetic grid voltage is derived. Both voltages are necessary because the PML needs to access both values [8, 9]. Furthermore, for a hybrid update, β and γ are transformed to the diagonal matrices $\mathbf{D}_\beta$ and $\mathbf{D}_\gamma$, where every grid edge can be assigned a specific value. For a more detailed explanation we refer to [5] which shows the analog procedure for a PML in z-direction. The hybrid implicit-explicit update for a face PML in ρ direction is given by

$$\begin{aligned}
\widehat{\mathbf{h}}^{n+\frac{1}{2}} &= \mathbf{A}^{-1}\Big(\mathbf{D}_{h_1}\Big(\mathbf{D}_{h_2}\widehat{\mathbf{h}}^{n-\frac{1}{2}} \quad (4)\\
&\quad -\Delta t \mathbf{M}_\mu^{-1}\left(\left(\mathbf{C}(\mathbf{D}_\beta \mathbf{D}_{e_1}\mathbf{D}_{e_2}) + \mathbf{C}\mathbf{D}_\eta\right)\widehat{\mathbf{e}}^n\right.\\
&\quad +\mathbf{C}\mathbf{D}_\xi \widehat{\mathbf{e}}^{n-1} + \Delta t \mathbf{C}\mathbf{D}_\beta \mathbf{D}_{e_1}\mathbf{M}_\varepsilon^{-1}\mathbf{C}^T\mathbf{M}_{\sigma_n}\Psi^{n-\frac{1}{2}}\\
&\quad \left.+\mathbf{C}\mathbf{M}_{\kappa_n}\Phi^n - \Delta t \mathbf{C}\mathbf{D}_\beta \mathbf{D}_{e_1}\mathbf{M}_\varepsilon^{-1}\widehat{\widehat{\mathbf{j}}}^n\right)\Big)\Big),\\
\Psi^{n+\frac{1}{2}} &= \Psi^{n-\frac{1}{2}} + \Delta t \widehat{\mathbf{h}}^{n+\frac{1}{2}}, \quad (5)\\
\widehat{\mathbf{e}}^{n+1} &= \mathbf{D}_{e_1}\Big(\mathbf{D}_{e_2}\widehat{\mathbf{e}}^n + \Delta t \mathbf{M}_\varepsilon^{-1}\Big(\mathbf{C}^T\widehat{\mathbf{h}}^{n+\frac{1}{2}} \quad (6)\\
&\quad +\mathbf{C}^T\mathbf{M}_{\sigma_n}\Psi^{n+\frac{1}{2}} - \widehat{\widehat{\mathbf{j}}}^n\Big)\Big),\\
\Phi^{n+1} &= \Phi^n + \Delta t \widehat{\mathbf{e}}^{n+1}, \quad (7)
\end{aligned}$$

with the abbreviations

$$\begin{aligned}
\mathbf{A} &= \mathbf{I} + \Delta t^2 \mathbf{D}_{h_1}\mathbf{M}_\mu^{-1}\mathbf{C}\mathbf{D}_\beta\mathbf{D}_{e_2}\mathbf{M}_\varepsilon^{-1}\mathbf{C}^T \quad (8)\\
&\quad +\Delta t^3 \mathbf{D}_{h_1}\mathbf{M}_\mu^{-1}\mathbf{C}\mathbf{D}_\beta\mathbf{D}_{e_2}\mathbf{M}_\varepsilon^{-1}\mathbf{C}^T\mathbf{M}_{\sigma_n},
\end{aligned}$$

$$\mathbf{D}_{h_1} = \left(\mathbf{I} + \frac{\Delta t}{2}\mathbf{M}_{\sigma_{t1}}\right)^{-1},\ \mathbf{D}_{h_2} = \left(\mathbf{I} - \frac{\Delta t}{2}\mathbf{M}_{\sigma_{t1}}\right), \quad (9)$$

$$\mathbf{D}_{e_1} = \left(\mathbf{I} + \frac{\Delta t}{2}\mathbf{M}_{\kappa_{t1}}\right)^{-1},\ \mathbf{D}_{e_2} = \left(\mathbf{I} - \frac{\Delta t}{2}\mathbf{M}_{\kappa_{t1}}\right), \quad (10)$$

$$\mathbf{D}_\eta = \frac{1}{2}\mathbf{I} - 2\mathbf{D}_\beta + \mathbf{D}_\gamma, \quad \mathbf{D}_\xi = \frac{1}{2}\mathbf{I} + \mathbf{D}_\beta - \mathbf{D}_\gamma. \quad (11)$$

$\mathbf{I}$ is the identity matrix, and the additional degrees of freedom Φ and Ψ correspond to the integrals of the electric and magnetic grid voltages over the simulated time, respectively. The diagonal matrices $\mathbf{M}_{\sigma_n}$, $\mathbf{M}_{\sigma_{t1}}$, $\mathbf{M}_{\kappa_n}$ and $\mathbf{M}_{\kappa_{t1}}$ contain the artificial material of the PML. Normal components carry the index n and are here the z-components. Tangential components have the index $t1$ and are in this case the ρ and ϕ components. For $\beta = 0$ and $\gamma = 0.5$ the update reduces to the ordinary Leapfrog scheme. Regarding the memory requirements in comparison to the standard PML, there are only two additional $\widehat{\mathbf{h}}$ and $\widehat{\mathbf{e}}$ vectors (at previous time steps) to store within the PML region. Additionally, the inversion of the Matrix $\mathbf{A}$ has do be performed once. As the matrix is sparse and diagonal, an efficient LU factorization usually is available.

3 Numerical Evaluation

We analyze an empty circular structure that is open in ρ direction. Its height is $h = 2\,\mathrm{m}$, and it is terminated by perfect electric conducting (PEC) walls in the $\pm z$-direction and a PML in ρ-direction at $a = 30\,\mathrm{m}$, see Figure 1. The hybrid implicit-explicit time-domain update is performed on a cylindrical grid using the body of revolution ansatz on a 2.5-D grid. The excitation is realized by a current source in the center of the cavity and only has a single non-zero

z-component. It is driven by a sinus modulated Gaussian pulse with bandwidth $74\,\text{MHz} \leq f \leq 184\,\text{MHz}$. This will excite cylindrical waves propagating in ρ-direction. Note that the longitudinal PEC boundaries lead to a waveguide-like propagation characteristic with a mixture of different modes, most of them with a typical cut-off behavior.

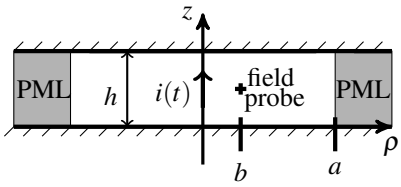

Figure 1. Sketch of the circular structure with PML in ρ-direction.

3.1 Stability Chart

To evaluate the stability of the hybrid algorithm, the parameters β and γ are systematically varied within the PML region, while a standard leapfrog procedure is used in the remaining region. As already shown in [5], the implicit algorithm is always unstable for $\gamma < 0.5$, corresponding to a forward time-stepping scheme. Therefore β and γ are varied in the range of $0.5 \leq \gamma \leq 1$ and $0 \leq \beta \leq 1$. Here, a PML with 12 layers and reflectivity of $\mathscr{R} = 10^{-4}$ (as target values) is used. The abort criterion is set to the maximum number of iterations of $500,000$. In all stable simulations, the energy of the simulation already reached the numerical noise level, before the maximum of iterations. In Figure 2 the resulting stability chart is depicted. For comparison with the longitudinal z-PML, the stability graph for a PML in z-direction, with 3 layers and $R = 10^{-2}$ from the previous publication [5] is repeated in Figure 3. The computed example was a hollow circular waveguide with PML in the propagation direction.

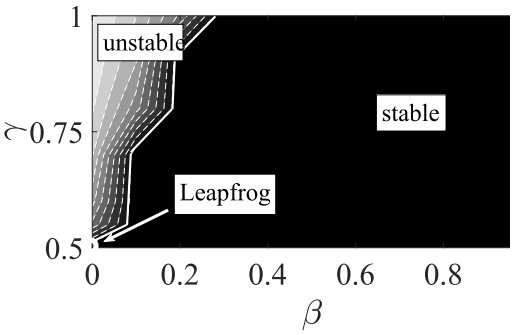

Figure 2. Stability chart for the local Newmark-beta parameters β and γ for a ρ-PML with 6 layers and $\mathscr{R} = 10^{-4}$. A darker color depicts a higher number of stable time steps.

As expected, the simulation is unstable for some parameter values, characterized in the chart by the lighter colors and separated from the stable area by a white line. In contrast to the previous results for the longitudinal PML, we can now state that for the radial PML the 'leapfrog point'

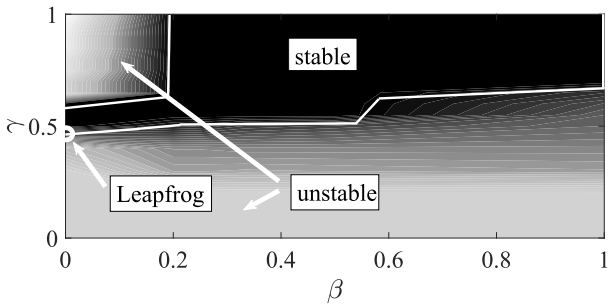

Figure 3. Stability chart for the local Newmark-beta parameters β and γ for a z-PML with 3 layers and $\mathscr{R} = 10^{-2}$. The model problem is a circular hollow waveguide with PML in propagation direction, from [5].A darker color depicts a higher number of stable time steps.

lies clearly within the stable region. Furthermore, only the unstable region of the ρ-PML (for $\gamma > 0.5$ and small β) is similar to the one of the z-PML, whereas the other unstable parameter sets from the z-PML do not cause stability problems for the ρ PML. This suggests that the ρ-PML causes significantly fewer problems of instability than the z-PML, especially concerning to the standard Leapfrog method.

3.2 Reflection coefficient

In the following, the reflection coefficient R and its dependence on the PML parameters is investigated. Different values for the number N_{lay} of PML layers and the target value for the reflectivity $\mathscr{R}$ are tested, and the Newmark-beta parameters β and γ are varied in the range of $0 \leq \beta \leq 1$ and $0.5 \leq \gamma \leq 1$. The reflection factor is determined by recording the fields at a point in the computational area with a field probe, see Figure 1. Based on the length in radial direction, a distinction between incoming and reflected pulse is possible. These two pulses are separately Fourier transformed, and the reflection factor R is defined as the ratio of their amplitudes at the frequency $f = 100\,\text{MHz}$ in some distance to the cutoff frequency of the first and the second mode.

In Figure 4 and Figure 5 the computed reflection coefficient R is shown for different β and γ, with $\mathscr{R} = 10^{-4}$. Figure 4 shows the result for 6 and Figure 5 for 12 layers of PML. In case of an unstable simulation, no reflection coefficient is computed.

Both results show, that there exists some influence of β and γ on the PML performance which, however, is hard to predict in advance. In none of the setups the requested reflected reflectivity is achieved in the real simulation. This is probably caused by a combination of different effects, including the dispersion characteristics and cut-off phenomena of the involved radiation modes, the neglected metric expressions in the PML coefficients, and the limited grid resolution in both tangential and normal direction. Nevertheless, the simulation with 12 layers of PML achieves slightly lower values for the reflection R.

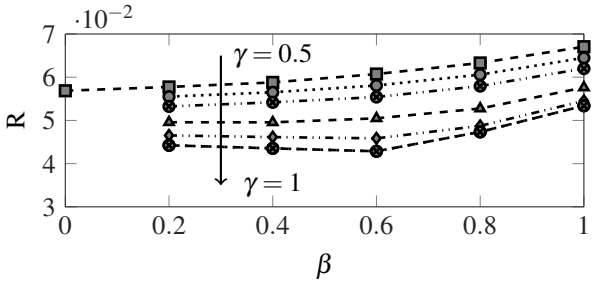

Figure 4. Reflection R for 6 PML layers and $\mathscr{R} = 10^{-4}$ coefficient for different $\beta \in [0,1]$ and $\gamma \in [0.5,1]$.

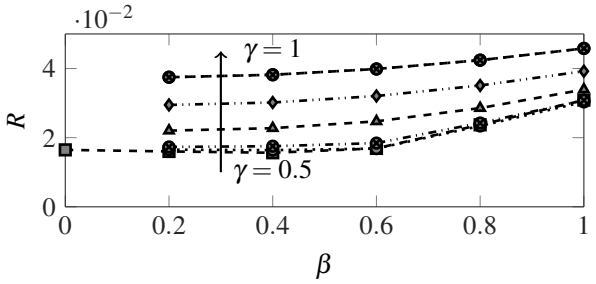

Figure 5. Reflection R for 12 PML layers and $\mathscr{R} = 10^{-4}$ coefficient for different $\beta \in [0,1]$ and $\gamma \in [0.5,1]$.

To compare the influence of the reflection coefficient $\mathscr{R}$ in dependence of the number on PML layers, the reflection is recorded for 12, 6 and 3 layers with $\gamma = 0.5$. In Figure 6 the reflection R is shown in dependence of β for different numbers of layers, with $\mathscr{R} = 10^{-4}$ (solid graph) and $\mathscr{R} = 10^{-2}$ (dashed graph).

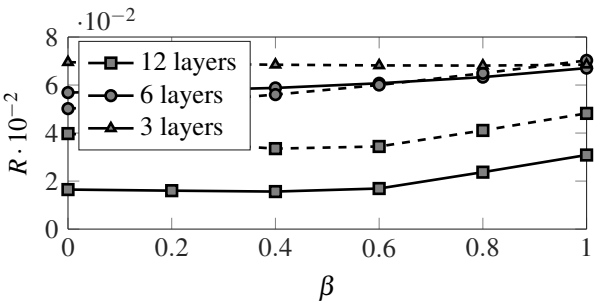

Figure 6. Reflection R for different amount of PML layers, dependent on β with $\gamma = 0.5$. The solid graph corresponds to $\mathscr{R} = 10^{-4}$ and the dashed graph to $\mathscr{R} = 10^{-2}$.

It can be seen that the reflection factor R improves with an increasing number of PML layers.

4 Conclusion

We analyzed a hybrid implicit-explicit time domain scheme with a radial PML with respect to its stability properties, the measured reflection at the boundary, and the computational cost. A circular structure with an absorbing boundary condition in the ρ-direction served as an example. Compared to the PML in the z-direction, the PML in the ρ-direction has fewer unstable zones in the stability graph. The existing unstable areas are almost congruent with parts of the unstable areas of the z-PML. Additionally, the Leapfrog update scheme is no longer in an unstable area. Thus, the ρ-PML has fewer problems with unstable behavior than the z-PML, and the parameter sets from z-PML can be used in both cases (and probably also in combinations of both.) Furthermore, it can be stated that the reflection at the boundary condition is influenced by the parameters β and γ of the implicit method. As expected, a larger number of PML layers improve its absorbing behavior, where, however, the target values are not reached for the given waveguide-like setup with its typical cut-off effects. Although the implicit calculation within the ρ-PML seems to be not mandatory for a stable time integration, it remains an interesting option, since no deterioration of the reflection values are observed. This makes the hybrid scheme a promising candidate for the important case of a combination of both PML boundaries, where the source of any instabilities will be harder to detect and to assign to a specific region of the grid.

References

[1] J.-P. Bérenger, "A perfectly matched layer for the absorption of electromagnetic waves," *J. Comput. Phys.*, vol. 114, no. 2, pp. 185–200, 1994.

[2] F. L. Teixeira and W. C. Chew, "On causality and dynamic stability of perfectly matched layers for FDTD simulations," *IEEE Trans. Microw.Theory Tech.*, vol. 47, pp. 775–785, 1999.

[3] N. Fang and L.-A. Ying, "Stability analysis of Yee schemes to PML and UPML for Maxwell equations," *J. Comp. Math.*, pp. 729-747, 2009.

[4] L. Kuen, P. Jorkowski and R. Schuhmann, "Spectral stability of PML implementations in time domain for resonators with radiation losses," *in Proc. ICEAA*, Verona, 2017, pp. 1387–1390.

[5] L. Kuen and R. Schuhmann, "Study on the stability of Perfectly Matched Layer implementations using a hybrid imlicit-explicit update scheme," *IEEE Transactions on Magnetics*, vol. 56, no. 2, pp. 1-4, 2020.

[6] T. Weiland, "Time domain electromagnetic field computation with finite difference methods," *Int. J. of Num. Modelling*, vol. 9, no. 4, pp. 295-–319, 1996.

[7] N.M. Newmark, "A method of computation for structural dynamics," *in Proc. ASCE*, 1959, pp. 67–94.

[8] T. Rylander and A. Bondeson, "Stability of explicit–implicit hybrid timestepping schemes for Maxwell's equations," *J. Comput. Phys.*, vol. 179. no. 2, pp. 426–438, 2002.

[9] S. Kirsch and R. Schuhmann, "A locally implicit FDTD scheme with relaxed time step constraint for non-uniform meshes," *in Proc. of EMTS*, 2016, pp. 133–136.